

PACS 68.35.-p, 73.20.-r

Electron states at the Si-SiO₂ boundary (Review)

V.E. Primachenko, S.I. Kirillova, V.A. Chernobai, E.F. Venger

V. Lashkaryov Institute of Semiconductor Physics, NAS of Ukraine,

41, prospect Nauky, 03028 Kyiv, Ukraine

E-mail: pve_18@isp.kiev.ua; phone: +38 044 525 6332

Abstract. This review is aimed at analysis of the system of discrete and continuously distributed boundary electron states (BES) on (111) and (100) silicon surfaces in the Si-SiO₂ structures prepared mainly using thermal oxidation of silicon. Used here are literature data as well as results obtained by authors when studying the temperature and electric field dependencies of the capacitive photovoltage. It has been ascertained that the BES system consists of a continuous U-like distribution in the silicon forbidden gap and from the discrete BES as well. There developed are two discrete BES in the thermally oxidized Si(111)-SiO₂ structure, while in the Si(100)-SiO₂ structure – four ones. These results well coordinated with ESR investigations were obtained using the method of temperature dependencies for capacitive photovoltage without application of an external electric field. As shown, application of various electric-field methods enables to determine only effective parameters of discrete and especially continuously distributed BES, which depend on the temperature of measurements, silicon resistivity and conditions of preparation of the Si-SiO₂ boundary. Considered are the features of pre-oxidation treatment of the silicon surface and its oxidation, the character of the intermediate layer between Si and SiO₂, and the influence of such external factors as annealing in various ambient atmospheres, irradiation and high electric fields as well.

Keywords: electron states, conductivity.

Manuscript received 09.07.05; accepted for publication 25.10.05.

1. Introduction

Electron states at a surface (interface) of solids were predicted in theoretical works by Tamm [1] and Shockley [2]. For the first time, these states were experimentally observed in the experiments made by Shockley and Pearson [3] who tried to influence with external electric field on the conductivity of Ge and Cu₂O thin films, *i.e.*, to realize the idea of metal-dielectric-semiconductor (MDS) transistor. Originally, there was a failure in creating this transistor, which was related to strong screening the electric field by surface states, but the method providing the influence of the external electric field on the semiconductor conductivity later named as “field effect” found its wide applications in studying the system of surface (boundary) electron states (SES or BES) [4-6].

The idea of MDS-transistor was realized only after a considerable decrease in the density of electron states on the silicon surface by growing here an oxide layer due to high-temperature oxidation of silicon in oxygen atmosphere [7, 8]. This thermally grown oxide layer not

only decreased the density value of BES at the boundary oxide-silicon (SiO₂-Si) by two – three orders, but appeared to be rather perfect dielectric layer, which, after covering this layer with a metal one, provided creation of the unique system – metal-oxide-semiconductor (MOS) successfully functioning for more than forty years in various devices of silicon electronics (transistors, varicaps, integrated circuits, CCD, *etc.*). Therefore, a huge amount of works (see, *e.g.*, [9-14]) were devoted to investigations of thermally oxidized silicon surface as well as to that after applying various methods for deposition oxide and other dielectric films onto this surface.

Despite the relatively low density of BES at the Si-SiO₂ boundary, which allows the external electric field to change the charge carrier concentration in the sub-surface area of the silicon MOS system, these BES, however, exercise a negative influence on operation efficiency of MOS devices. For example, BES increase the noise of transistors and integrated circuits based on MOS-systems, decrease the efficiency of charge transfer in CCD as caused by generation-recombination

processes with BES participation (especially in CCD without a hidden transfer channel), promotes degradation of MOS-systems operating at high voltages and radiation of various types [9-14]. Therefore, a considerable part of works is devoted to investigations of the nature of BES at the boundary Si-SiO₂, determination of their parameters, as well as to changing the latter due to the influence of various technological factors, namely: conditions of a pre-oxidation treatment, technology of thermal oxidation and post-oxidation annealing in vacuum or some gas atmosphere. There investigated are BES parameters after various mechanical strains at the Si-SiO₂ boundary and high electric voltages as well as radiation exposures applied to the MOS-system. All these investigations are aimed at the BES nature, understanding of which will enable to eliminate these states or, at least, to reduce their influence to some minimum.

Predominant majority of methods to investigate the BES system is based on applying an external electric field to the boundary Si-SiO₂, which enables to determine BES parameters via measurements of the surface capacity, conductivity or photovoltage [9] due to changes in filling the boundary states with charge carriers. The external field is also applied when using the methods allowing to measure temperature dependencies of the surface capacity (the Gray-Brown method [15] and in the method of deep-level transient spectroscopy (DLTS) [16]. In our opinion, in these investigations studied is not only the system of the so-called fast BES but also partly the electron states located in the oxide film and, first of all, in its junction layer due to various mechanisms of electrotransfer between these electron states and bulk silicon, which is inherent both to electrons and holes. It complicates interpretation of experimental results and determination of BES parameters by using these data.

In [17-21], to study the BES system we offered the method for measuring temperature dependencies of the surface (capacitive) photovoltage, when the external electric field was not applied to the system Si-SiO₂. It enables to determine parameters of fast BES located at the silicon substrate. The obtained results are in good agreement with the data of investigations of paramagnetic centers in the silicon substrate, which was obtained using electron spin resonance (ESR) [22]. Performed simultaneously investigations of the photovoltage dependence on the value of the external electric field applied to the system Si-SiO₂ at various temperatures showed that in this case determined are the parameters of effective BES located both on the silicon substrate and in the SiO₂ layer [19, 21]. In this work, we analyze the results of investigations of the BES system that are obtained by us as well as numerous authors using the structures Si(100)-SiO₂ и Si(111)-SiO₂. Besides, we have briefly considered the response of the BES system on various actions applied to the Si-SiO₂ structure.

2. Preparation of the Si-SiO₂ system by using thermal oxidation of silicon

In relation with the tendency to increase the density of MOS-structures located on the unit of IC area, dimensions of MOS-structures in microelectronics are gradually lowered, which requires obtaining a thin (unities or tens of nanometers) gate insulator SiO₂ layer with a defectless structure [14]. Therefore, there formed rather hard requirements to the process of preparing the thermally oxidized Si-SiO₂ system. A considerable attention is paid to pre-oxidizing treatment of silicon plates, which mainly determines quality of the sub-gate SiO₂ layer. The oxidized silicon surface should possess no structural defects, be close to atomically smooth surface and contain no harmful impurities (metal, carbon, *etc.*). Managed to realize something like to this surface by using several steps in liquid chemical treatment of silicon plates [23, 24]. The prepared by them surface was covered by the hydrogen monolayer and possesses a number of advantages over the atomically clean surface prepared and kept in super-high vacuum [23] not only from the viewpoint of more simple and convenient technology for making IC but also in relation to its higher cleanness and structural perfection as compared to the atomically clean surface prepared in vacuum. At first, silicon plates cut from monocrystalline ingots are treated with chemical-mechanical polishing in alkaline solutions (KOH or NaOH) to eliminate mechanical damages in the surface area that arise during the cutting process and to provide a flat polished surface. The following treatment is carried out using highly pure chemical reagents and deionized water to avoid contamination of the plate surface with harmful impurities, especially metal ions that are adsorbed by silicon [25].

One of the reliable ways to clean the plate surface from metal impurities and hydrocarbons is ten-minute treatment of them in the mixture H₂O₂:NH₄OH:H₂O = 1:1:5 at 80 °C with the following rinse in deionized water (RCA treatment) [23]. At the following stage, they use various methods for slight preliminary oxidation of the plates (with chemical reagents, thermal processing in O₂ atmosphere or photooxidation in ozone atmosphere). This stage is aimed at oxidation of the subsurface layer containing structural defects after chemical-mechanical polishing, with the purpose of its following scalping. The scalping of this oxidized layer can be performed in water HF solutions with various concentrations (possibly with NH₄OH additions) [23, 24], or in solutions of NH₄F [23] as well as HBF₄ [26].

It was found that after treatments in HF, NH₄F or HBF₄ silicon surface is protonized and possesses remarkable properties. Using various methods, namely, IR spectroscopy, scanning tunnel microscopy, low electron diffraction, photoelectron spectroscopy, ellipsometry, electron energy loss spectroscopy, *etc.*, it was revealed that this silicon surface is passivated with

hydrogen, contains hydrides of various types (Si-H, Si-H₂, Si-H₃) and is close to the atomically smooth one, with Si-H bonds being dominant on even parts. Si(111) and Si(100) surfaces are not reconstructed, do not contain superlattices from surface silicon atoms as it is usually observed at atomically clean surfaces prepared in vacuum. These hydrogen-passivated surfaces are hydrophobic [23, 24] and are not oxidized for a long time in dry oxygen and water that does not contain dissolved oxygen. The shelf time under ambient conditions for this surface can exceed several hours and is rather sufficient to transfer silicon plates into the chamber for thermal oxidation.

Creation of hydrogen-silicon bonds after treatments in HF, NH₄F and HBF₄ instead of the silicon-fluorine ones seemed unexpected at the very beginning as the Si-F bond energy is close to 6 eV while that for the Si-H bond is 3.5 eV [23, 24]. A reasonable explanation for the process of protonized Si surface formation was offered in [23, 24, 28]. In the Si-F bond, the electron is mainly shifted from the Si atom to the F one ($\delta = 0.7$), while in the Si-H bond this transfer is much weaker ($\delta = 0.18$). As a result, SiF₄ molecules created first on the silicon surface are easily picked off the substrate silicon atoms due to solvation by water molecules, while these silicon atoms, in their turn, are profitably bound to hydrogen. However, after treatments of silicon in above mentioned fluorine acids there remain fluorine-hydrogen silicon compounds on its surface (e.g., SiH₂F₂, SiHF₃), which requires short-time (less than 10 s) processing of these silicon plates in deionized water (without dissolved oxygen, as a rule) in order to provide complete elimination of fluorine compounds and creation of surface passivated only with hydrogen. It is noteworthy that the treatment of silicon surface in concentrated HF solutions (with low pH) results in more rough protonized surface than that in diluted HF solutions or in NH₄F and HBF₄ solutions. Usually, in industrial conditions used are the following solutions: HF:NH₄F = 1:7 or 40 % NH₄F with pH = 5 and 7, 8 [23].

When placing protonized silicon plates into the chamber for thermal oxidation, hydrides are easily desorbed with increasing temperature. Thermal desorption of monohydrides is observed at 200 °C, dihydrides – at 400 °C and trihydrides – at 550 °C [23]. There exist various methods to prepare SiO₂ films [9-14]. However, the only thermally grown film is suitable for preparation of sub-gate dielectric. Earlier, to prepare it various technologies were used, too. For example, to neutralize various impurities easily diffusing in SiO₂ (in particular, sodium), these impurities being accumulated at the boundary Si-SiO₂, used were the technologies with addition of chlorine, phosphorus, lead [9]. At lower temperatures, SiO₂ layers with an adequate thickness were realized by addition of vapor into oxygen atmosphere. However, in recent years after reaching a technological purity when growing the SiO₂ layer, used is oxidation in dry oxygen that does not contain any

impurities, as the latter beside a positive influence provide the negative one on the SiO₂ properties as well as on operation of MOS-structures in some cases.

Currently, thin films of SiO₂ gate insulator are grown in dry O₂ atmosphere within the temperature range 800 to 950 °C. As it was ascertained in [29], the most resistant to electric breakdown are the films oxidized at 850 °C independently from their thickness within the interval 3.5 to 5 nm. However, despite the more than 40-year period of successful applications of SiO₂ films as a gate insulator, the works to develop their preparation technology are in progress. So, for instance, some authors managed to prepare SiO₂ films with good parameters in dry O₂ at lower temperatures due to using ultra-violet (UV) [30] or excimer lamp radiation [31]. Although in the latter case the oxidation temperature was only 250 °C, the breakdown field reached (7...10)·10⁶ V/cm, the films possessing the low density of the built-in positive charge. SiO₂ films prepared with UV radiation in dry oxygen at 600 – 900 °C possess a higher breakdown voltage, lower leakage currents and trap levels for holes when injecting them into the films as compared to the SiO₂ films obtained after their standard oxidation in dry O₂. Taking into account that structural and electric defects at the Si-SiO₂ boundary are caused by structural mismatch between Si and SiO₂, authors of [32] offered the method to realize stationary oxidation of silicon when the quantity of these defects is reduced to minimum. As the growth of the SiO₂ film takes place due to diffusion of oxygen through the previously created SiO₂ film [9], to keep oxidation stationarity it is offered to regulate either the oxidation temperature or the partial oxygen pressure.

3. Study of electron states at the Si-SiO₂ boundary

The most widely spread methods to investigate BES system at the boundary Si-SiO₂ are voltage-capacity $C(V)$ measurements, DLTS as well as studying the dependencies of the transverse conductivity in MOS-structures (impedance active component) in various frequency ranges $G(\omega)-V$ [9-14, 22, 33-36]. The $C(V)$ -method enables to determine BES concentration and their energy-scale location inside the silicon forbidden gap, while DLTS and $G(\omega)-V$ methods, in addition, provide determination of the capture cross-section for majority carriers by BES, but to spread the investigation over the whole forbidden gap it is necessary to consider both *n*- and *p*-Si.

Most of the investigations were made using thermally oxidized structures Si(111)-SiO₂ and Si(100)-SiO₂. As usual, the Si(100)-SiO₂ structure possesses lower BES concentration, smaller built-in positive charge inside the SiO₂ film at the boundary and higher performances of MOS-systems based on it, therefore it is this structure that is used in IC production [9-14]. Although application of different methods to the same structure often results in different figures, it is possible

to make some general conclusion about the BES system. It is ascertained that there is a common background of the continuous U-like BES distribution inside the silicon forbidden gap with increased concentrations near the edges of v - and c -bands. The BES concentration in this U-like distribution can change within wide limits from $1 \cdot 10^9$ up to $1 \cdot 10^{13} \text{ cm}^{-2} \text{ eV}^{-1}$ in dependency on technology of manufacturing the Si-SiO₂ structure. Besides, the above methods allows to found discrete levels below and above the middle of the silicon forbidden gap E_i with concentrations within the range $1 \cdot 10^{10}$ to $1 \cdot 10^{13} \text{ cm}^{-2} \text{ eV}^{-1}$, which can be observed in the background of the U-like distribution as broad peaks [22, 33-36]. Maximums of these BES peaks both for Si(111)-SiO₂ and Si(100)-SiO₂ structures are located at 0.3 and 0.85 eV above the edge of silicon v -band [33-36].

In parallel with electric investigations of the BES system, in works [22, 33, 34] performed was studying the electron-spin resonance (ESR) in these Si-SiO₂ structures. Using the structure Si(111)-SiO₂, the authors of [33] revealed the ESR signal from the so-called P_b center, comprehensive investigations of which [22] enabled to ascertain that it is located at the silicon surface and is a defect represented by a boundary silicon atom related to three Si atoms from the layer below, while one of its dangling bonds is oriented along the perpendicular to (111) plane. The P_b center is designated as $\text{Si}_3 \equiv \text{Si} \bullet$ defect. As it was shown by investigations of dependencies of the P_b center ESR signal on the electrical voltage applied to the MOS-structure, the ESR signal is decreased when the Fermi level at the silicon surface is located closer than 0.3 eV to the v -band and further than 0.85 eV from it. In the former case the defect $\text{Si}_3 \equiv \text{Si} \bullet$ loses the unpaired electron and become positively charged, while in the latter case it catch one electron more and become negatively charged. Both positively and negatively charged P_b centers do not yield the ESR signal. Juxtaposition of ESR and DLTS results shows that the P_b center is an amphoteric defect that creates two levels in the silicon forbidden gap, the distance between them being close to 0.55 eV and serving as an effective correlation energy for the centers with broken bonds at the boundary Si-SiO₂. It is well confirmed by simultaneous decrease of two peaks in the BES density determined with DLTS and the concentration of ESR centers when annealing MOS-structures in vacuum for 15 min within the temperature range 150 – 350 °C. The annealing at 450 °C (30 min) results in full decay of these ESR centers, concentration of which before this processing was $1.5 \cdot 10^{12} \text{ cm}^{-2}$ [33].

Although the investigations of $C(V)$ -dependencies [34], the $G(\omega)-V$ ones [35], both of these dependencies in combination with DLTS [36] by using the Si(100)-SiO₂ structure yield the positions of discrete BES density peaks inside the forbidden gap practically the same as for the Si(111)-SiO₂, ESR investigations of the Si(100)-SiO₂ boundary reveal two paramagnetic centers: P_{b0} и P_{b1} [34]. While the P_{b0} center is identical to P_b center at

the (111) surface and also creates levels at the distance 0.3 and 0.85 eV above the v -band edge, the P_{b1} center creates levels at the distances 0.45 and 0.80 eV above v -band and possesses the correlation energy value only 0.35 eV. For a long time, the nature of the P_{b1} center remained unclear and was under discussion. It was assumed, for example, that it is a center of $\text{Si}_2\text{O} \equiv \text{Si} \bullet$ type [22, 34]. At last, in [37] it was ascertained that the P_{b1} center like to the P_{b0} center is the defect $\text{Si}_3 \equiv \text{Si} \bullet$ where oxygen is not its part but the broken bond of this defect has another orientation relatively to the (100) surface, namely, it is directed at the angle 20° to the axis $\langle 011 \rangle$. Thus, the only different orientation of the broken bond inherent to defects $\text{Si}_3 \equiv \text{Si} \bullet$ yields different positions of energy levels in the silicon forbidden gap.

As it was noted in [34], one can observe a correlation between the energy distribution of BES and the total distribution of levels created by P_{b0} and P_{b1} centers. But the concentration of BES is approximately two times larger than the total concentration of P_{b0} and P_{b1} centers. It means that P_{b0} and P_{b1} defects represent only a part of BES, parameters of which are determined by the $C(V)$ -method. As it is assumed in [13, 22], the reason of it lies in the possibility to control filling the electron states not only on the silicon surface where these states are created by P_{b0} and P_{b1} defects but electron states inside the intermediate layer of the Si-SiO₂ boundary, if using the $C(V)$ -method. It is confirmed by our measurements of temperature (without any applied external voltage) and field (at various temperatures) dependencies for the surface photovoltage that will be analyzed in the following chapter. Moreover, our investigations enabled to separately determine parameters of energy levels created by P_{b0} and P_{b1} defects, which could not be done with $C(V)$, $G(\omega)-V$ and DLTS methods.

Concluding this chapter, it is reasonable to consider the question about the capture cross-sections by BES value of which can be determined by $G(\omega)-V$ [35] and DLTS [36] methods. As noted in [35], there are discrepant data in literature. For instance, applying the method $G(\omega)-V$ to the n -Si(100)-SiO₂ structure it was obtained that the capture cross-section reduces by two orders from 10^{-14} cm^2 down to 10^{-16} cm^2 for BES distributed from E_i up to the c -band edge. For the p -Si(100)-SiO₂ structure, it was obtained that the cross-section by BES for holes changes from 10^{-16} cm^2 down to 10^{-17} cm^2 when the BES position changes between 0.25 and 0.05 eV starting from E_i . At the same time, the DLTS method yields in the independent from BES position value 10^{-14} cm^2 for the capture cross-section of holes. Analyzing their own data obtained for the temperature range 300 – 100 K, authors of [35] made the conclusion that the capture cross-sections for electrons and holes do not depend on temperature and BES position inside the forbidden gap and are approximately equal to 10^{-16} cm^2 . By contrast, authors of [36] state that for holes the capture cross-sections have a considerable

dependency on temperature. In our opinion, these differences in data both in quantitative and even in qualitative relations as regards to the capture cross-sections for carriers by BES in various BES positions and temperatures of measurements can be explained, on the one hand, by limitations of the used methods [36] and their incorrect use as well as, on the other hand, by the fact that these methods control not only BES on Si surface but inside the SiO₂ subsurface layer, that is dependent on SiO₂ technology.

4. Investigation of BES by surface photovoltage method

In our works, to study the BES system at thermally oxidized surfaces *n*-Si(100) [19, 21] and *p*-Si (100) [20] we used the method of the surface (capacitance) photovoltage at a high generation level of electron-hole pairs in silicon excited by a light pulse capable to flatten energy bands at the boundary Si-SiO₂. It enabled to determine the boundary potential ϕ_s in silicon in darkness (before illumination) under various temperatures and external electric fields when applying the latter to the Si-SiO₂ structure. It is noteworthy that the Dember photovoltage at high generation levels of charge carriers by the intense light pulse (10^{21} quanta/cm²s) does not play any essential role due to comparable values of diffusion coefficients as a consequence of electron-hole scattering [38].

Temperature dependencies of ϕ_s within the range 300–100 K were taken using a cryostat with a measuring capacitor consisting of the sample with a mica insulator covered with a semitransparent conducting layer SnO₂(Sb). In the course of lowering the temperature, at its definite value we could observe the effect of photomemory for ϕ_s [25], therefore ϕ_s measurements were performed by the first light pulse complying the procedure of cleaning out the surface traps from trapped minority charge carriers [39]. Electric field dependencies $\phi_s(V)$ were measured under definite fixed temperatures within the range 300–100 K. The external voltage V applied to the measuring capacitor was varied between +400 to –400 V. In this case, the measurements were carried out under illumination of the capacitor with the second light pulse in their train to eliminate the influence of the ϕ_s photomemory effect by saturation of the traps with minority charge carriers created by the first light pulse as well as to avoid nonequilibrium arising in silicon at depleting voltages V [40].

Depicted in Fig. 1 are the dependencies $\phi_s(T)$ for thermally oxidized (curve 1) and chemically oxidized in HNO₃ (curve 2) surfaces *n*-Si(100). The curves 3 and 4 correspond to $\phi_s(T)$ dependencies obtained after removing the oxide layers from surfaces in HF solutions. Negative ϕ_s values correspond to existence of subsurface layers depleted with electrons. The growth of $|\phi_s|$ with decreasing the temperature is caused by filling the BES with electrons as a consequence of the Fermi level shift

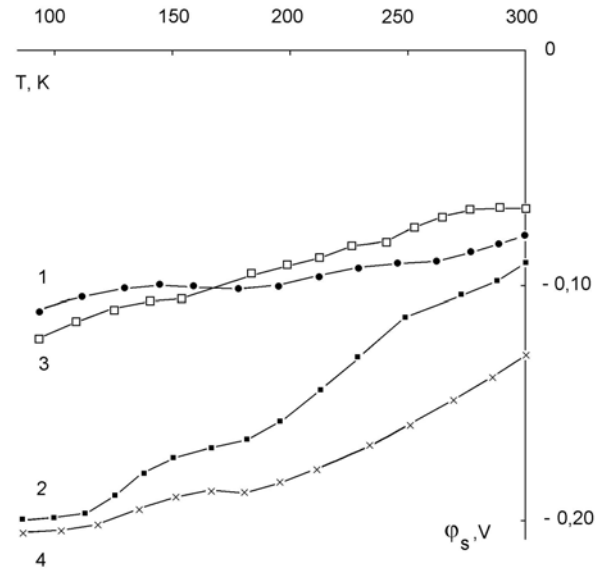


Fig. 1. Temperature dependencies of the surface potential for thermally (1) and chemically (2) oxidized silicon that was then treated in HF (curves 3 and 4, respectively).

to the c-band. The definite ϕ_s value is corresponded by the charge Q_{sv} in the silicon subsurface region that is equal to [9, 25]:

$$Q_{sv} = \sqrt{2} q n_i L \{ \lambda^{-1} [\exp(q\phi_s/kT) - 1] + \lambda [\exp(-q\phi_s/kT) - 1] + q\phi_s/kT(\lambda - \lambda^{-1}) \}^{1/2}, \quad (1)$$

where $L = (\varepsilon\varepsilon_0 kT/q^2 n_i)^{1/2}$, $\lambda = n/n_0$, n_0 and n_i are electron concentrations at the temperature T inside the bulk of the studied and intrinsic silicon, respectively, q is the electron charge, ε is the silicon dielectric constant, k is the Boltzmann constant, $\varepsilon_0 = 8.85 \cdot 10^{-12}$ F/m. The charge Q_{sv} taken with the opposite sign is equal to the total charge Q_s trapped in BES. When going from $Q_s(T)$ dependencies to the $Q(\psi_s)$ ones where $\psi_s = \phi_b + \phi_s$, the ϕ_s value is measured and ϕ_b value is determined for every T from the condition $n_0 = n_i \exp(q\phi_b/kT)$. The values $q\phi_b$ and $q\psi_s$ are equal to the energy distance between E_i and the Fermi level inside the silicon bulk and on its surface, respectively. The $Q_s(\psi_s)$ dependence allows to determine the density N_{sf} of fast BES available at the silicon surface at various $q\psi_s$ (or energies E inside the forbidden gap relatively E_i) in the following form:

$$N_{sf}(E) = |\Delta Q_s| / \Delta(q\psi_s). \quad (2)$$

Fig. 2 shows the obtained $N_{sf}(E)$ dependencies corresponding to surfaces characterized with the $\phi_s(T)$ dependencies shown in Fig. 1. It is seen that the least BES density at the thermally oxidized surface (curve 1) that is corresponded to two observed BES density peaks at energies $E_i + 0.23$ and $E_i + 0.32$ eV with concentrations $6 \cdot 10^{10}$ and $3.4 \cdot 10^{10}$ cm⁻²eV⁻¹. The largest BES density is observed on the chemically oxidized surface (curve 2).

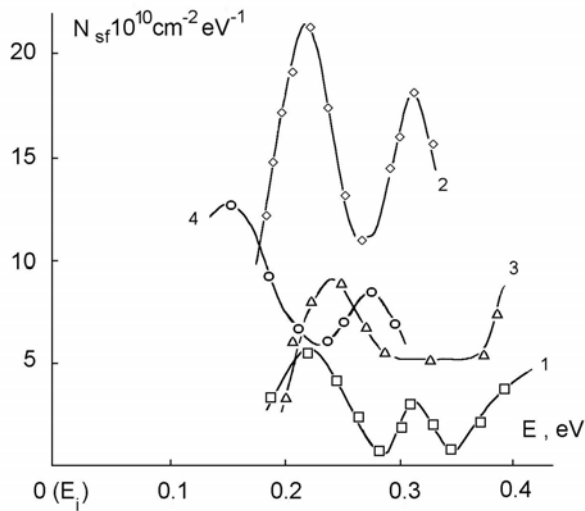


Fig. 2. Distribution of the density N_{sf} of fast BES vs the energy above the middle of the silicon forbidden gap E_i . 1 and 2 denotes thermally and chemically oxidized Si surfaces; 3 and 4 – the same surfaces after their treatment in HF, respectively.

Also observed here are two density peaks possessing the same energy position as for the thermally oxidized surface within the accuracy 0.01 eV but with larger corresponding concentrations: $2.2 \cdot 10^{11}$ and $1.8 \cdot 10^{11} \text{ cm}^{-2} \text{ eV}^{-1}$. The identical energy position of the found discrete BES both on thermally and chemically oxidized n -Si(100) surfaces is indicative of the same nature of defects causing their creation on these surfaces. We assume that these defects are P_{b0} and P_{b1} centers.

As seen from Fig. 2, after HF-treatment applied to the thermally oxidized surface the BES density grows a little (curve 3), while that of the chemically oxidized surface is lowered (curve 4). Also changed in this case are the energy positions of the BES density. The latter is obviously related with the fact that after HF-treatment, water rinsing and some exposure in ambient atmosphere, these are covered with hydrogen SiH_x compounds and contain residual Si-F bonds as well as Si-OH and Si-O bonds creating in air, as it was shown earlier [23, 24]. Atoms H, F, O or OH-groups located near the $\text{Si}_3\equiv\text{Si}\bullet$ defects that remain non-passivated with hydrogen can result in changing the position of energy levels created by these defects [13]. Note that if the n -Si(100) surface thermally oxidized and then treated in HF to leave for aging in air, then already after 7 days the BES concentration increases and reaches values characteristic for the chemically oxidized surface, while in 22 days when a real relatively stable oxide is created [41, 42] it even exceeds these values [19]. In this case, the energy position of the BES density peak located closer to E_i gradually becomes more close to E_i with aging [19]. Thus, one can observe not only the growing concentration of $\text{Si}_3\equiv\text{Si}\bullet$ defects but also changing the energy positions of the levels created by them when aging the surface treated in HF and then acquiring the real oxide layer.

To determine BES parameters inside the bottom part of the silicon forbidden gap, in the work [20] we obtained temperature dependencies of the photovoltage inherent to thermally oxidized p -Si(100). We studied p -Si(100)-SiO₂ structures with thicknesses of SiO₂ equal to 90 and 3 nm. It was shown that in both cases we deal with discrete levels located below E_i by 0.11 and 0.22 eV. Thus, the thermally oxidized (100) surface contains the system of discrete levels with the following energy positions: $E_i-0.22$, $E_i-0.11$, $E_i+0.23$ and $E_i+0.32$ eV. The energy positions of middle levels ($E_i-0.11$ and $+0.23$ eV) coincide with those of created by P_{b1} centers developed in ESR investigations [34] with the accuracy 0.01 eV. The extreme levels ($E_i-0.22$ and $+0.32$ eV) are close to those created by P_{b0} centers ($E_i-0.26$ and $+0.29$ eV, respectively [34]). This difference 0.03–0.04 eV between our results and those obtained in [34] can be related with worsening the accuracy of surface potential determination from $C(V)$ -measurements when band bends are large. But note that the correlation energy value for the P_{b0} center is the same both in our work and in [34].

Thus, the method of photovoltage temperature dependencies without applying any external electric field allowed to separately develop the levels created by P_{b1} and P_{b0} centers on the thermally oxidized (100)Si surface. Before our works, it did not manage to do that with various electric or photoelectric methods. Then was an opinion that P_{b1} centers do not create levels in the forbidden gap, which could manifest themselves in electric measurements [43]. However, in the work [44] where spin-dependent recombination (SDR) of charge carriers at the Si(100)-SiO₂ boundary was investigated applying the variable voltage to a MOS-structure, it was shown that this recombination occurs through both P_{b0} and P_{b1} centers, *i.e.*, the latter are located in the silicon forbidden gap. However, to determine energy level positions for P_{b0} and P_{b1} , as it was done in our work, the SDR method could not manage, because it yields very broad signal lines.

As it follows from the above results, the use of methods even with little (differential) voltages applied to the MOS-structure is accompanied with a partial capture of charge carriers by electron states in the oxide film, at least in its intermediate layer with silicon. An essential growth of this capture was also observed in our works [19, 21] where dependencies of the capacitance photovoltage were measured under various temperatures as a function of high Π -pulse voltage V applied to the measuring capacitor possessing the specific capacitance C_d . In this case, to obtain the BES density distribution inside the silicon forbidden gap, we used the $\varphi_s(V)$ dependencies that allows to calculate the BES density for various φ_s according to the formula [45]:

$$N_s(\varphi_s) = [C_d(dV/d\varphi_s - 1) - dQ_{ss}/d\varphi_s]/q. \quad (3)$$

As it was done above, $N_s(\varphi_s)$ dependencies obtained for a definite temperature allow to obtain the $N_s(\psi_s)$ ones or,

what is the same, $N_s(E)$ dependencies. Shown in Figs 3 and 4 are the dependencies $N_s(E)$ for thermally and chemically oxidized n -Si(100) surfaces, respectively, measured within the temperature range 290 down to 130 K. For the thermally oxidized surface, the BES concentration N_s within the energy interval $-0.2...+0.2$ eV relatively to E_i does not depend on the temperature of measurements and lies within the limits $(2...4) \cdot 10^{11} \text{ cm}^{-2} \text{ eV}^{-1}$. The dependency of N_s on temperature is observed within the range 0.2 to 0.5 eV above E_i . A sharp growth of N_s at more high temperature begins at lower E (or $\psi_s = \varphi_s + \varphi_b$). It takes place when to silicon surface one applies the electric fields capable to enrich the subsurface area with electrons and to rise φ_s . The φ_s – values for which N_s grows sharply are approximately the same at various temperatures. And the observed shift of the N_s growth beginning into the side of higher E -values with increasing the temperature is caused by the growth of φ_b from 0.28 eV at 290 K up to 0.47 eV at 130 K.

If comparing the dependencies $N_{sf}(E)$ and $N_s(E)$ (Figs 2 and 3) obtained for the same thermally oxidized surface by using two different approaches, one can see that, first, the character of the BES distribution differs: the $N_{sf}(E)$ dependencies possess a discrete structure, while the $N_s(E)$ ones show a continuous BES distribution. Second, the BES concentration determined using the $\varphi_s(T)$ dependencies is more than 10 times less as compared to N_s determined from the $\varphi_s(V)$ -dependencies at various temperatures. It is related with the fact that the N_{sf} value determined in absence of external electric field is only equal to the concentration of true fast BES located on the silicon surface in the Si-SiO₂ structure. At the same time, when using the electric-field method to obtain the N_s value one can observe supplementary BES located in the near-boundary (intermediate) area of SiO₂ film, as there is a considerable electric field promoting transfer of charge carriers between silicon and the oxide BES.

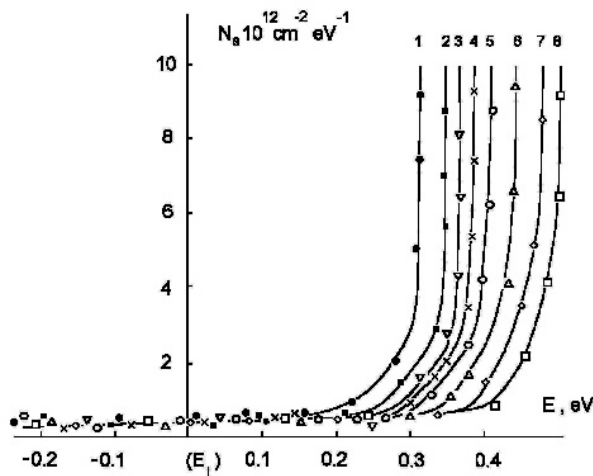


Fig. 3. Distribution of the effective BES density N_s vs the energy for the thermally oxidized Si surface at various temperatures: 1 – 290, 2 – 270, 3 – 255, 4 – 230, 5 – 205, 6 – 185, 7 – 150, 8 – 130 K.

When inducing the charge Q_{ind} on silicon surface at the initial moment before changing the charge in BES, the electric field inside the oxide film ξ_s is as follows:

$$\xi_s = Q_{\text{ind}} / \varepsilon_d \varepsilon_0 = [Q_{\text{sv}}(\varphi_{s0}) - Q_{\text{sv}}(\varphi_s)] / \varepsilon_d \varepsilon_0, \quad (4)$$

where φ_{s0} and φ_s are the silicon surface potentials before and after application of an external electric field to it, respectively, ε_d is the silicon oxide dielectric constant. When $\varphi_s > 0$, the charge Q_{sv} is negative, while for $\varphi_s < 0$ it is positive.

According to formulae (1) and (4), the electric field in the oxide film ξ_s is in proportion to $|q\varphi_s/kT|^{1/2}$ when the external field voltage depletes silicon with electrons. In our experiments, ξ_s reaches $3 \cdot 10^4$ V/cm. A sharp growth of ξ_s takes place, if one applies enriching voltages: $\xi_s \sim \exp(q\varphi_s/kT)$. In the case of low temperatures, this sharp growth is observed at high $E \equiv q\psi_s$ [46], as it follows from the formulae (1) and (4). Thus, there is a correlation between the dependencies $\xi_s(E)$ and $N_s(E)$ in the enriched region: the larger ξ_s is corresponded by the larger effective BES density, ξ_s and N_s being dependent on the temperature of measurements. Effectively, the correlation between $\xi_s(E)$ and $N_s(E)$ explains the results of the work [47]. There, for the first time in investigations of the field effect (that is the influence of an external electric field on the subsurface conductivity of germanium and silicon), attention was turned to the correlation between dependencies of the charge in BES and that in the subsurface semiconductor region on φ_s when changing the semiconductor resistivity and temperature of measurements.

Among various possible mechanisms of electron transfer between silicon and electron states in oxide [9, 10], an essential role can be played by the tunnel mechanism of transfer from the silicon c-band into oxide states located in the vicinity of the Si-SiO₂ boundary, if the voltages are enriching.

Immediately after applying the electric field to the Si-SiO₂ structure, the rate of tunnel filling with electrons some kind oxide states with the concentration N_{i0} can be expressed as

$$dn_{i0} / dt \sim DC_{no}(N_{i0} - n_{i0}) v_s n_s, \quad (5)$$

where n_{i0} is the concentration of electrons in oxide states, C_{no} is the effective capture cross-section for electrons by these states, $n_s = n_0 \exp(q\varphi_s/kT)$ is the electron concentration in the c-band near Si surface, v_s is their thermal velocity, D is the transmission coefficient for electrons in the space of the thickness d between Si and oxide states, which is equal

$$D = D_0 \exp\{-4/3 \sqrt{2} m / \hbar [(U - E_n)^{3/2} - (U - q\xi_s d - E_n)^{3/2}] / q\xi_s\}, \quad (6)$$

where $D_0 \approx 1$, and U is the height of the potential barrier at the Si-SiO₂ boundary, E_n – the energy of tunneling electrons, m – electron effective mass in oxide, \hbar – the Planck constant divided by 2π .

As it follows from the formulae (5) and (6), in the case of enriching voltages electron tunneling into the oxide states grows considerably due to increasing D and n_s values. As seen from calculations, the latter factor is especially essential, because n_s grows exponentially with φ_s . Electron tunneling results in a considerable growth of the effective BES density determined from the electric-field photovoltage investigations, while the true density of fast BES N_{sf} determined from photovoltage temperature dependencies within the range 0.2 up to 0.4 eV above E_i is more than ten times less in its magnitude (Figs 2 and 3). Note that when measuring the photovoltage temperature dependencies (without any external electric field) the silicon forbidden gap is studied in the regime of depletion of the surface with electrons. In this mode, electron tunneling from Si into oxide states does not take place via the absence of the electric field in oxide, which is capable to promote tunneling and due to low n_s values.

As seen from Fig. 4, in the case of chemically etched in HNO_3 silicon surface the effective density N_s considerably grows as compared to that for thermally oxidized surface. It is related both with a large quantity of defects creating electron states in the oxide film and with an increasing probability of charge carrier transfer between these states and silicon due to various transfer mechanisms [9, 10]. When removing the chemically oxidized film by etching in HF, N_s values are considerably reduced at definite E and T values, which is indicative of the fact that just the states in the chemically

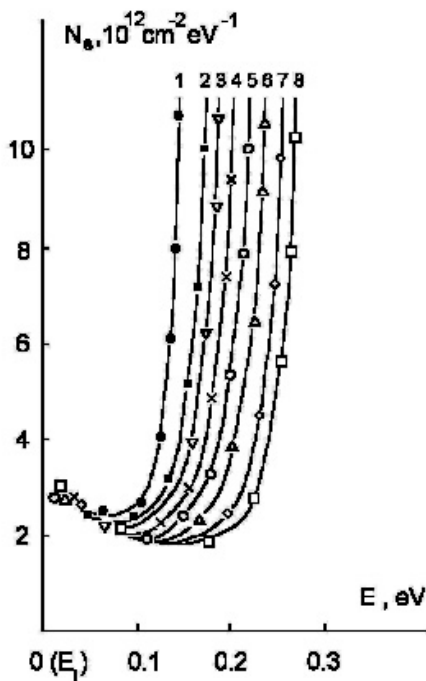


Fig. 4. Distribution of the effective BES density N_s vs the energy on the chemically oxidized Si surface at various temperatures: 1 – 290, 2 – 270, 3 – 255, 4 – 230, 5 – 205, 6 – 185, 7 – 150, 8 – 130 K.

oxidized film mainly contribute into determined effective N_s values. Note that the $N_s(E, T)$ values were practically the same after etching both chemically and thermally oxidized films. Thus, as it follows from electric field photovoltage investigations at various temperatures, the determined distribution of the efficient BES inside the silicon forbidden gap depends both on the state of the oxide film on the silicon surface and on measurement temperatures as well as the silicon resistivity (parameter φ_b).

The latter inference allows to make the conclusion that improvement of MOS-transistor functions (that is a decrease of a harmful influence of BES) requires not only a structurally perfect Si-SiO₂ boundary with a low defect concentration both in it and the SiO₂ film but a moderate silicon resistivity of MOS-structures as well as lowered operation temperatures for MOS-transistors.

5. Intermediate layer at the Si-SiO₂ boundary and U-like dependency of the BES density

In the majority of works studying the structure and electrophysical properties of the Si-SiO₂ system, intimated is the presence of an intermediate layer between Si and SiO₂, which consists of near-boundary Si and SiO₂ layers more or less smoothly transforming one to another and possessing properties that differ, respectively, both from those of Si bulk and SiO₂ [9-14]. For 40-year history, the thickness of the thermally grown insulating SiO₂ layer has been reduced from hundreds of nanometers to the values less than 4 nm [14]. In accord with these technological achievements, the thickness of measured intermediate layer has been decreased from 3...5 nm to parts of nanometer. As this takes place, one can note vanishing some its definite properties and domination of others. To study this intermediate layer, used was a powerful arsenal of various methods, namely: the optical ones (various methods of infrared (IR) and ultraviolet (UV) spectroscopy, monochrome and spectral ellipsometry, light electroreflectance, optical microscopy, etc.); X-ray methods (X-ray imaging, photoelectron spectroscopy); electron-beam methods (electron diffraction, Auger-electron spectroscopy, electron-energy characteristic loss spectroscopy, transmission electron microscopy, reflection electron microscopy); ion-beam methods (Rutherford back-scattering spectroscopy, mean energy range ion spectroscopy, secondary-ion mass-spectroscopy); scanning tunnel microscopy, electron-spin resonance, etc. [9-14, 25, 48]. The intermediate layer was investigated both directly in Si-SiO₂ structures with a various thickness of the SiO₂ film and in the course of thinning the SiO₂ film in a slowly etching HF solution or when sputtering it with an ion beam.

It was ascertained that the determined thickness of the intermediate layer depends both on the technology of the SiO₂ film preparation and on the methods of its investigations. Thermal oxidation of silicon stimulates

break of Si-Si bonds (energy per one bond is equal to 1.97 eV) that is followed by creation of more fast Si-O bonds (energy per one Si-O bond in SiO₄ tetrahedron is equal to 5 eV). Energy released in these reactions promotes creation of structural defects in the silicon subsurface region possibly up to its partial amorphization. Besides, the silicon subsurface region is enriched with imbedded oxygen, concentration of which can exceed the solubility limit in silicon bulk [9]. In addition, one can also observe accumulation of various impurity atoms at the Si-SiO₂ boundary where they gather both from the silicon side and from the side of growing SiO₂ layer. Therefore, to create more perfect Si-SiO₂ boundary, technology of its preparation was advanced by elimination of impurity atom influence and reducing the amount of structural defects created in the silicon near-boundary region. It has been successfully realized providing super-high purity conditions for growing the SiO₂ layer, using super-high purity reagents, choosing an optimum temperature and regimes for silicon oxidation as well as post-oxidizing annealings [9-14]. But works in this direction are going on. For example, as noted in [30, 31], works to lower oxidation temperatures for silicon are carried out.

It was shown using the listed above methods that the SiO₂ film grown on silicon is amorphous but can include some microcrystalline inclusions, especially in the vicinity of the intermediate layer [9, 48]. The base of all the SiO₂ crystalline and amorphous modifications is formed by silicon-oxygen tetrahedra SiO₄, the bond length and valence angles of which does not practically depend on the type of modification and are equal to 0.16 nm and 109°, respectively [48]. In SiO₂ amorphous films, the short-range order is conserved, and angles between SiO₄ tetrahedra change within the wide range from 120 up to 180° with the maximum of their distribution close to 147°. In SiO₂ amorphous film bulk, SiO₄ tetrahedra mainly form 6- and 4-link rings, the 4-link ones being dominant in the vicinity of the boundary [49]. A smaller angle between tetrahedra is a characteristic feature for bridge bonds in these 4-link rings.

Availability of microcrystalline SiO₂ inclusions near the boundary was mainly observed in more thick SiO₂ films in insufficiently pure conditions for their growth, when various impurities (in particular, sodium atoms or ions [9]) become crystallization centers for SiO₂. Currently, they are absent in insulator SiO₂. However, the intermediate SiO₂ layer is enriched with silicon (or, in other words, depleted with oxygen). It is considered that there are suboxides of the following types Si₂O₃, SiO and Si₂O near the boundary from the SiO₂ side, which is capable to explain oxygen deficiency. As it was ascertained in [50], where oxygen films with the thickness 2.4 nm were studied, the thickness of suboxide layer was only 0.2 nm, *i.e.*, the boundary between Si and SiO₂ is close to the very sharp one. These suboxides consist of Si-O_x-Si_{4-x} type silicon-oxygen clusters ($1 \leq x < 4$) [51] that possess angles in bridge Si-O-Si

bonds less than those between silicon-oxygen tetrahedra in SiO₂ bulk, which manifests itself in red-shifted bands observed in IR spectra.

Besides, electrophysical and ESR methods found point structural defects in SiO₂ near-boundary region (for example, E-, S-, EH- and EX-centers) [9-13, 48, 52-54]. These centers serve as capture centers for electrons and holes and can manifest themselves in various electrophysical investigations of electron states inside the Si-SiO₂ boundary, in particular, when applying electric field to it, which has been considered by us above. Possible intrinsic defects in SiO₂ that can serve as capture centers for electrons and holes have been analyzed in [55]. In particular, electrons and holes can be captured by E'-center that is the O₃≡Si• defect. This defect is assumed to be responsible for appearance of the built-in positive charge in oxide near the Si-SiO₂ boundary in the course of silicon thermal oxidation [9]. Note that the built-in positive charge is inessential when the SiO₂ thickness is less than 4 nm [14]. The role of electron traps can be also played by proton-containing defects (*e.g.*, Si-OH and Si-H groups) [48], which is especially typical for oxides prepared in wet medium. Thus, there are specific intermediate regions both from the silicon and SiO₂ sides at the Si-SiO₂ boundary.

The intermediate region in the Si-SiO₂ structure is considerably affected by internal mechanical strains (IMS) [56-61]. There are two main reasons of IMS appearance, namely: i) structural mismatch between silicon and the growing oxide film, which results in compressive strains in oxide arising in the process of thermal oxidation, while in near-boundary silicon layers stretching strains (intrinsic IMS) take place; ii) difference between coefficients of thermal expansion for oxide and silicon ($5 \cdot 10^{-7} \text{ K}^{-1}$ and $3 \cdot 10^{-6} \text{ K}^{-1}$, respectively), which yields in an increased level of IMS in the Si-SiO₂ structure when cooling it from the oxidation temperature to that of application (or the room one). The intrinsic IMS are approximately equal to 70 % of the total IMS value [59]. As the thickness of the SiO₂ film is usually much less than that of the silicon substrate, the IMS value in the SiO₂ film is essentially higher than in the substrate. The former reaches $(2-6) \cdot 10^8$ Pa, while the latter is approximately 10^7 Pa. This latter value is far from the ultimate stress limit $(2-4) \cdot 10^9$ Pa [58], but is close to the beginning of the microflow process in silicon, which is realized in the case of thick SiO₂ films [60]. These strains in the silicon substrate are sufficient, at least, to create point defects at the silicon boundary and enhance this process when applying high electric voltages to the Si-SiO₂ structure or exposing it to various kinds of radiation [61, 62]. It is noteworthy that from the analysis of possible conjugation between Si and SiO₂ lattices as well as from experimental data [51], it follows that IMS at the boundary Si(111)-SiO₂ are higher than those at the Si(100)-SiO₂ boundary. As a consequence, there observed a larger amount of created point defects of the P_b center type on the silicon surface with (111) orientation [22].

After this consideration of intermediate layer properties at the Si-SiO₂ boundary and IMS inherent to it, let us turn to U-like background of BES density distribution in the silicon forbidden gap, on which the BES created by P_b centers manifest themselves. The BES concentration in this U-like distribution also depends on technology of Si-SiO₂ structure preparation, but the nature of these BES differs from that of the BES created by P_b centers. The former are usually observed near c- and v-bands of silicon and practically do not change, for instance, after low-temperature (up to 450 °C) annealings in vacuum, as it takes place with BES created by P_b centers [22].

For the first time, notions about the nature of the U-like BES distribution were developed in the works [63, 64] by using the concept of a disorder available at the semiconductor-dielectric boundary. It was assumed in [64] that the reason of these BES appearance lies in considerable oscillations of effective charge values on Si and O atoms in the intermediate layer SiO₂, and this fluctuating charge yields in creation of this U-like distribution of BES on silicon surface, if using the theory of disordered systems [65]. The charge fluctuation on Si and O atoms is caused by fluctuations of angles in Si-O-Si bridge bonds of boundary silicon-oxygen tetrahedra SiO₄ and clusters Si-O_x-Si_{4-x}. This angle fluctuation arise in the course of Si-SiO₂ structure creation and is enhanced by IMS.

A direct confirmation of above considerations was obtained from the studying the boundary region of the Si-SiO₂ structure by using highly-resolving X-ray photoelectron spectroscopy [66]. The model explicated above is also supported by theoretical works [67, 68]. In [67], using the method of Bette lattices shown was that angle variations of Si-O-Si bonds at the boundary result in creation of BES density tails near c-bands of Si and SiO₂, while variations of Si-Si bonds available in the near-boundary oxide layer cause creation of the BES density tail near the Si v-band as well as tails in the SiO₂ forbidden gap. Using the same method, it was obtained in [68] that even ideal contact between silicon and oxide lattices cause state tails in the silicon forbidden gap near c- and v-bands.

In summary, it is worth to note that although these U-like distributed BES negatively effects on operation of MOS-devices, the deeper BES (created by P_b centers) are rather more harmful as they supplementary serve as generation-recombination centers for electron-hole pairs.

6. Influence of external factors on the BES system

6.1. Annealings of Si-SiO₂ structures

Usually, when creating the MOS-structure, deposition of the metal layer (or polysilicon) is followed by their annealing at relatively low temperatures (< 450 °C). This annealing in vacuum provides good adhesion of the metal layer to SiO₂. Besides, annealing at relatively low temperatures decreases IMS in the Si-SiO₂ system to

some extent, eliminates many structural defects in the intermediate Si-SiO₂ layer, shortens its thickness, and reduces the BES concentration as well [9]. As it was mentioned above, in [33] BES created by P_b centers practically vanished after low-temperature annealings in vacuum. In contrast, the annealing in vacuum at higher temperatures (> 600 °C) more significantly decreases IMS at the boundary owing not only to changing the Si-O-Si bond angles in the intermediate layer but to creation of the point defects of the P_b center type on the silicon surface, *i.e.*, one can observe a growth in the BES concentration [69]. Besides, high-temperature (> 700 °C) annealings in vacuum cause degradation of the oxide film via creation of point defects in it, which can be determined using the ESR method [53]. Thus, to reduce the BES concentration one should use the only low-temperature annealings in vacuum. The possible mechanism providing the decrease in the BES concentration due to neutralization of P_b centers in this case was offered in [70]. It was shown being based on theoretical calculations that passivation of silicon broken bonds caused by creation of Si=O double bonds in conditions of oxygen deficiency (vacuum annealing) stimulates displacement of levels created by P_b centers from the forbidden gap into extended bands, which means that BES disappear from the forbidden gap.

Taking into account that in some cases it is necessary to do high-temperature annealings of the Si-SiO₂ structure (for example, to reduce the concentration of the built-in positive charge in oxide) in [71] they investigated the high-temperature annealing (1000, 1100 or 1160 °C) of Si-SiO₂ structures not only in vacuum but in various gas atmospheres (He, Ne, Ar, N₂) as well. It was ascertained that the vacuum annealing increases the concentration of BES stemming from P_b centers and results in degradation phenomena in SiO₂, namely: an increased conductivity of SiO₂ even at low voltages applied to the MOS-structure; enhanced sensitivity of SiO₂ to radiation that generates a higher concentration of hole traps. Annealings in Ne, Ar and N₂ atmospheres were able to eliminate some of the considered above negative phenomena inherent to the structure after the vacuum annealing, however, the best result was obtained for He atmosphere. The annealing in He resulted in practically full elimination of above negative phenomena. The authors assumed that it takes place due to embedding the small-size He atoms into oxide and especially into the Si-SiO₂ boundary, which prevents chemical reactions between Si and SiO₂ as well as creation of point defects at Si-SiO₂ boundary.

A large amount of works (*e.g.*, see [72-78]) were devoted to passivation of P_b centers caused by the annealing of Si-SiO₂ structures in hydrogen atmosphere providing disappearance of levels related to BES stemming from P_b centers. In [72, 73] studied was the passivation kinetics of P_b, P_{b0} and P_{b1} centers at the Si-SiO₂ boundary in the course of the annealing in H₂ atmosphere within the temperature range 213 – 234 °C.

It is assumed that passivation of P_b , P_{b0} and P_{b1} centers is caused by the reaction $\text{Si}_3\equiv\text{Si}\cdot + \text{H}_2 \rightarrow \text{Si}_3\equiv\text{SiH} + \text{H}$. Values of the activation energy for this reaction are practically the same for P_b , P_{b0} and P_{b1} centers and are equal to 1.51, 1.51 and 1.57 eV, respectively, which is not a surprise as P_b and P_{b0} centers located accordingly on (111) and (100) silicon surfaces are identical, while the P_{b1} center on (100) surface differs from P_{b0} centers only by the orientation of the silicon atom broken bond. $P_b\text{H}$, $P_{b0}\text{H}$ and $P_{b1}\text{H}$ complexes created in the course of passivation are rather unstable. They decay during the annealing in vacuum at temperatures ≥ 500 °C, and are very unstable under radiation influence as well as high electric voltages applied to MOS-structures [74]. In [75], authors offered a theoretical model for thermal dissociation of the above complexes in (111) and (100) Si-SiO₂ structures taking into account diffusion of hydrogen atoms and molecules into SiO₂ provided by annealings in vacuum within the temperature range 480 – 700 °C. This model has a good accordance with experimental data. It is essential to note that the activation energies for hydrogen deliberation from $P_b\text{H}$, $P_{b0}\text{H}$ and $P_{b1}\text{H}$ complexes are equal to 2.78, 2.86 and 2.91 eV, respectively.

There are some distinctions in behavior of atomic hydrogen H as compared to the molecular one H₂ if regards to P_b centers [74, 76, 77]. As shown in [76], in contrast to H₂ the atomic hydrogen is able not only to passivate but also de-passivate silicon broken bonds even at room temperatures due to the following reactions: $P_b + \text{H} \rightarrow P_b\text{H}$ and $P_b\text{H} + \text{H} \rightarrow P_b + \text{H}_2$. It was ascertained in [77] that if at 400 °C atomic hydrogen passivates BES like the molecular one does, then at room temperatures (when H₂ is passive) it recovers the same defects that were present before their passivation with H or H₂. Besides creation of fast BES related mainly with silicon broken bonds, atomic hydrogen also forms traps (slow states) inside the SiO₂ film. In this case, the defects created by atomic hydrogen at the boundary and inside SiO₂ possess similar properties as compared to those of defects created by radiation as well as injected hot carriers [77]. Thus, in our opinion, passivation of silicon broken bonds with hydrogen (H and H₂) is not a reliable method to eliminate them. Moreover, as it was shown in [78], the annealing of the Si-SiO₂ structures in H₂ atmosphere at 450 – 800 °C results in creation of a considerable (up to 10^{13} cm⁻²) positive charge inside the SiO₂ film that is caused by the centers not providing any ESR signal.

In some relation, promising are the annealings in nitrogen-containing media (N₂, NO, N₂O). Processes that take place in this case yield in creation of Si/SiO_xN_y structures and are enlightened in more details in the review [14]. Our purpose is only to note some positive properties acquired by the Si-SiO₂ structure after nitrogeneing. As shown in [79], the concentration of P_b centers sharply drop after the annealing of the Si(100)-SiO₂ structure in NO (from $2 \cdot 10^{12}$ down to

$< 1 \cdot 10^{11}$ cm⁻²). It takes place due to NO penetration through SiO₂ to the Si-SiO₂ boundary with simultaneous appearance of built-in N and O atoms in it, which results in passivation of P_b centers without “harmful” effects of hydrogen. At the same time, dielectric properties of SiO₂ are kept.

As it was ascertained in [80], after annealing the Si(100)-SiO₂ structure in N₂ the nitrogen atoms embedded into the boundary lower IMS in the structure and increase stability of the boundary to trap generation during current loads. There observed some improvement of the Si(100)-SiO₂ boundary after annealing the sample at 900 °C N₂ atmosphere [81], namely, lowered is its roughness related to oxidation dynamics of (100) surface (the Si(111)/SiO₂ boundary is more smooth, and the annealing in N₂ has no effect on it). Note that roughness increases the BES concentration and built-in charge in oxide [82].

6.2. Radiation effects on the BES system

The existence of the intermediate layer containing IMS cause increased sensitivity of the Si-SiO₂ structure to various radiation effects [61, 62]. The structural transition from Si to SiO₂ through the intermediate layer where chemical bonds between atoms are strained and weakened results in a decreased threshold for defect creation as well as increased rate defect generation. In contrast to creation of radiation defects inside the Si or SiO₂ bulk, specificity of their creation at the boundary Si-SiO₂ is influenced by the following factors: elastic strains before radiation and their relaxation in the course of radiation; capability of atoms (ions) to move inside the boundary during radiation and after it; presence of electric fields inside the boundary (either applied from outside or caused by the built-in charge inside oxide) that like to IMS influence on atom (ion) displacements and, in such a manner, enhance structural reconstructions of the boundary as well as change the rate of chemical reactions in it.

Radiation actions on solids are caused by ionization losses of the energy or by elastic collisions of particles (photons) from the exposing beam interacting with atoms of solids [62]. When irradiation is realized by light quanta with various wavelengths, electrons, X-rays or gamma-quanta, the main channel for energy losses is ionization of atoms. In the case of ion-beam irradiation, besides atom ionization the dominant part of the ion energy is spent for elastic collisions with atoms that are shifted from their regular positions, especially when using more massive ions. Respectively, consequences of actions made by different kinds of radiation can be different.

If using radiation capable mainly to ionize atoms in conditions of moderate intensities of particle (quantum) fluxes and their energies, it is possible to realize the case when the structural reconstruction of the boundary stimulated by radiation results not only in decreased IMS inside the Si-SiO₂ boundary but in decreasing the

amount of defects in the intermediate layer, its ordering and improvement of MOS-structure electrophysical characteristics [83]. Bearing the above in mind, we used the method of photovoltage temperature dependences for studying the concentration and distribution of BES in the silicon forbidden gap in the n -Si(111)-SiO₂ structure in the course of its irradiation with nanosecond ruby laser pulses ($\lambda = 0.69 \mu\text{m}$) possessing the energy within the range $W = 0 - 1 \text{ J/cm}^2$ [18]. The respective energy of quanta is sufficient only for being absorbed in silicon with creation of electron-hole pairs. The latter interact with Si and O atoms in the intermediate layer, which results in its structural changes, including changes in the BES system. Figs 5 and 6 show, respectively, the distributions of the BES concentration N_{sf} in the silicon forbidden gap above E_i and the maximum BES concentration $N_{sf \text{ max}}$ after exposure of the studied structure to light pulses with various energies W . It is seen that for pulse energies less than 0.6 J/cm^2 the BES concentration is decreased, which means that one can observe the light annealing of BES.

Only for laser pulse energies reaching or exceeding the silicon melting energy ($W \geq 0.7 \text{ J/cm}^2$) one can observe an increase in the BES concentration. Fig. 5 also shows that in dependency on the energy of the irradiating pulse W the BES distribution in the forbidden gap changes. If before irradiation the $N_{sf \text{ max}}$ position corresponds to $E_i + 0.31 \text{ eV}$ (which is in satisfactory accordance with the energy position of the P_b center level [33]), then after irradiation with increasing W the position of $N_{sf \text{ max}}$ shifts first to the c-band side and then to E_i .

Possibly, a change of the structure around P_b center in the intermediate layer and/or the change of the broken

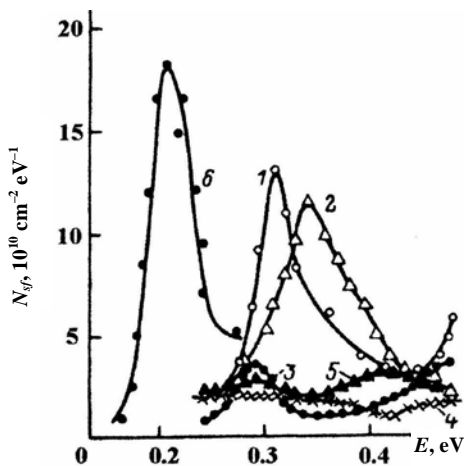


Fig. 5. Distribution of the BES density N_{sf} at the Si surface vs the energy E above E_i after action of laser pulses: 1 – unirradiated thermally grown Si-SiO₂ system; 2 to 6 – irradiated with the laser pulses energies 0.1, 0.2, 0.3, 0.6, 0.7 J/cm², respectively.

orbital orientation are responsible for these phenomena.

Irradiation of Si-SiO₂ structures with ionizing radiation possessing high quantum energies (UV, X-ray, gamma-radiation) in most of the cases yields an increased BES and defect (traps for charge carrier) concentrations in SiO₂, if one does not perform the following annealing. In works [84, 85], developed was the model of arising in the SiO₂ near-boundary area E' centers ($\text{O}_3 \equiv \text{Si} \bullet$ defect) and non-bridging oxygen due to broken by radiation strained Si-O bonds. Displacements of the non-bridging oxygen defect (and H atom) in electric and IMS fields to the boundary results in uncoupled Si-Si bonds and creation of P_b centers, *i.e.*, to the growth of the BES concentration. In [86], found was a good correlation between the E' center concentration and the positive charge in oxide, between the P_b center concentration and the BES density as well.

The structure Si-SiO₂ is unstable after radiation actions. ESR and spin-dependent recombination (SDR) investigations were carried out using MOS-structures with n - and p -channels (Si(100)-SiO₂ structure) after their irradiation with a proton beam possessing the mean energy 55 MeV or gamma-irradiation from the ⁶⁰Co source [88]. It turned out that immediately after any kind of above irradiations one can find only P_b centers and E' defects. However, after hundred-hours aging the irradiated structures, there observed P_{b1} -centers arising as a result of defect-transformation processes. The P_{b1}/P_{b0} center concentration ratio lay within the range 0–9 % in dependency on the time and conditions of aging. In particular, creation of P_{b1} centers is enhanced by positive voltage (+3 V) applied to the gate of the MOS-transistor. In the course of aging, the concentration of P_{b0} centers and E' defects was not practically changed.

One interesting effect more was observed in the work [89]. The authors investigated the distribution of the BES concentration after UV and X-ray irradiations by using the method of measurements of charge pumping currents in MOS-elements with n - and p -channels and polysilicon gates used in serial integrated circuits. In original MOS-elements (before irradiation) after standard production of IC, they observed only small tails of the BES density near c - and v -bands, *i.e.*, levels caused by P_b centers were absent. They did not appear after UV irradiation as well. If the MOS-elements are irradiated only with an X-ray beam ($5 \cdot 10^4 \text{ R}$), wide peaks of the BES density appeared above and below E_i in the range of P_b center levels with maximum concentrations $N_{sf} = (2 \dots 3) \cdot 10^{11} \text{ cm}^{-2} \text{ eV}^{-1}$. However, consecutive irradiation of these MOS-elements with UV light and then with the same X-ray beam ($5 \cdot 10^4 \text{ R}$) resulted in increasing the peak concentrations by more than the order of their magnitude ($> 3 \cdot 10^{12} \text{ cm}^{-2} \text{ eV}^{-1}$). This effect of a “hidden” preliminary influence of UV irradiation the authors explained by the following mechanism. UV irradiation releases hydrogen atoms at the boundary polysilicon-SiO₂, which diffuse to the Si-SiO₂ boundary and in the course of the following X-ray

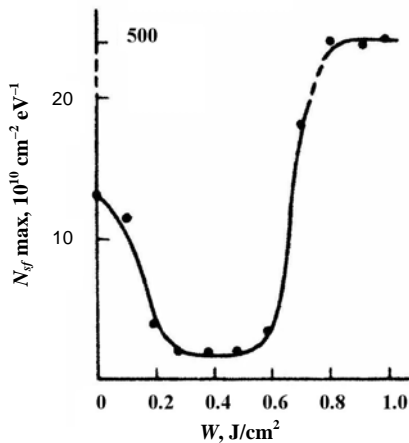


Fig. 6. Dependency of the peak Si BES concentration on the energy of laser pulses irradiating the Si-SiO₂ system.

irradiation take place in reactions resulting in P_b center creation. Note that the thermal annealing (150 °C, 30 min) between UV and X-ray irradiations eliminated the influence of preliminary UV irradiation, while the annealing at 400 °C (20 min) absolutely eliminates the BES created both after the only X-ray and consecutive UV+X-ray irradiation.

6.3. Influence of strong electric fields on the BES system

The BES system can be also transformed under the influence of electric fields applied to the MOS-structure in the course of its operation. Indeed, the SiO₂ film as well as intermediate layers of the Si-SiO₂ structure possess high internal electric fields, which results in creation of BES and defects in the SiO₂ film and, eventually, to full degradation of this film (its electric breakdown) [9-14]. The breakdown of a thick oxide layer ($d > 100$ nm) usually takes place in electric fields close to $8 \cdot 10^6$ V/cm, while considerable heating the charge carriers in their extended bands does at $(2 \dots 3) \cdot 10^6$ V/cm. The breakdown field for a thin oxide layer ($d \sim 3 \dots 4$ nm) is approximately $(2 \dots 3) \cdot 10^7$ V/cm as caused by destruction of Si-O bonds [90].

In the MOS-structure, when electric fields are sufficiently high but less than the breakdown ones, one can observe injection of charge carriers (electrons, holes) into SiO₂ both from silicon and the gate (consisting of metal or polysilicon). Being heated by electric field inside SiO₂, the injected carriers can create defects in SiO₂ and BES in silicon. In this case, there occur processes similar to those taking place in the MOS-structures under radiation exposure. In [91, 92], these processes were used to explain the BES density increase caused by avalanche injection of electrons and holes. It is

worth to note an essential role of IMS being present both at the boundaries Si-SiO₂ and gate(metal)-SiO₂.

Rather interesting results were obtained in [93], these were different in the cases of electron or hole injection. Using the method of charge pumping, the authors determined the BES density distribution on (100) silicon surface in *p*-channel MOS-transistors with the thickness of SiO₂ subgate layer equal to 7 nm after various technological procedures. Directly after MOS-structure creation without annealing them in H₂, the BES distribution possessed two broad peaks (above and below E_i) in the energy range of P_{b0} and P_{b1} centers. It is important to note that the method of charge pumping does not allow to separately determine levels created by P_{b0} and P_{b1} centers. Both peaks vanished after hydrogen passivation of these centers as a result of annealing them in H₂ atmosphere. The following injection of electrons into oxide, when the Fowler-Nordheim effect is valid, caused the predominant appearance of the BES above E_i , which means that the BES peak below E_i was not practically created. To explain the fact, it was offered the so-called “hydrogenic” model of BES activation for the states located above E_i : H atoms (or ions) released by hot electrons move to silicon surface and create broken silicon bonds in accordance with the reaction: $\equiv\text{Si-H}+\text{H}^+ + e \rightarrow \equiv\text{Si}\bullet + \text{H}_2$. However, if one realizes hole injection from silicon into oxide, there arose the BES peaks approximately equal in their magnitude not only above but below E_i , too. In this case, it is assumed that the reaction $\equiv\text{Si-H}+\text{hole} \rightarrow \equiv\text{Si}\bullet + \text{H} + \text{hole}$ is valid. The concentration of created BES increases with the level of hole injection but does not depend on the electric field strength in oxide E_{ox} within the range $(1 \dots 5) \cdot 10^6$ V/cm. The latter is in sharp contrast with the situation observed for electron injection, when increase in E_{ox} from $2 \cdot 10^6$ up to $4 \cdot 10^6$ V/cm enhanced generation of BES located above E_i by the order of value. This increase in the BES density with E_{ox} is conditioned by an increase of the electron energy, which results in larger amount of released hydrogen for the former of above mentioned reactions to be realized on silicon surface. At the same time, holes even at $E_{\text{ox}} = 5 \cdot 10^6$ V/cm remain insufficiently energetic to enhance hydrogen release in oxide, as their mobility here is 10^6 times lower than the electron one.

The authors of [93] conceive that the $\equiv\text{Si}\bullet$ defects obtained in reactions with hydrogen and hole participation differ, which results in doubled or single peaks in the silicon forbidden gap. It is not absolutely clear. Note in addition that another works demonstrated the fact that creation of the $\equiv\text{Si}\bullet$ defects due to splitting hydrogen from them in the course of high-temperature annealing lead to creation peaks both above and below E_i . Besides, known are the facts when at presence of the upper peak created by hot electrons or radiation the lower peak appeared after a long storage of the sample as a consequence of the intermediate layer structural transformation. In relation with it, remember that

transformation of the intermediate layer caused creation of the P_{b1} center, while immediately after radiation exposure only the P_{b0} centers were present [88]. As the broad peaks of the BES density above and below E_i include levels created by P_{b1} and P_{b0} centers, the way of BES creation due to electron or hole injection remains unclear. This is also complicated by the fact that separation of the hole and electron injection is very difficult sometimes, as it can take place simultaneously from the silicon substrate and from the gate of the MOS-system. It is noteworthy that hot holes are more efficient in BES generation than hot electrons at low levels of charge injection (below 10^{17} cm^{-2}), while the density of BES created by holes does not depend on the SiO_2 thickness but on the level of hole injection [94]. It is indicative of the fact that creation of BES by hot holes is the process inherent to Si boundary.

With a positive voltage on the MOS-structure gate possessing the thickness more than 4 nm, electron tunneling ensues from Si c-band into SiO_2 c-band through a triangular barrier (Fowler-Nordheim mechanism). However, when the SiO_2 thickness is about or lower than 3 nm, dominating is the direct tunneling of electrons from Si c-band into the gate by passing over SiO_2 c-band [14]. Besides, electron tunneling from BES into the gate is also possible [95]. These tunnel currents of electrons increase the total leakage current of the MOS-structures with thin SiO_2 layers and set the minimum possible for the SiO_2 thickness as 1.2 nm, which is sufficient to efficient operation of the MOS-devices. However, in [95] the real SiO_2 thickness in the efficiently operating MOS-structure was estimated as 3 nm. It is related with the considered in [95] recombination-tunnel mechanism of creating the BES by electrons, which results in the soft breakdown of SiO_2 .

When the dielectric thickness is tunnel-transparent, it is also impossible to form an inversion layer on silicon surface by using external electric field, as the minority charge carriers are extracted from silicon into the gate. Note in summary that many questions of studying the MOS-structures with SiO_2 layers thinner than 4 nm have been considered in the review [14] where it is shown, in particular, that oxide degradation (breakdown of the MOS-structures) may be caused by creation of BES and traps in this oxide due to an applied electric voltage.

References

1. I. Tamm, Uber eine mogliche Art der Elektronenbindung an Kristalloberflächen // *Phys. Z. Sowjetunion* **1**, p.733-736 (1932).
2. W. Shockley, On the surface states associated with a periodic potential // *Phys. Rev.* **56**, p. 317-320 (1939).
3. W. Shockley, G.L. Pearson, Modulation of conductance of thin films of semiconductors by surface charge // *Phys. Rev.* **74**, p. 232-236 (1948).
4. A. Many, Y. Goldstein, N.B. Grover, *Semiconductor surfaces*. John Willey and Sons, N.Y. (1965).
5. V.I. Lyashenko, V.G. Litovchenko, I.I. Stepko, *Electron properties on semiconductor surface*. Naukova dumka, Kiev (1968) (in Russian).
6. A.V. Rzhanov, *Electron processes on semiconductor surface*. Nauka, Moscow (1971) (in Russian).
7. M.M. Attalla, E. Tannenbaum, E.E. Schebner, Stabilization of silicon surfaces by thermally grown oxides // *Bell Syst. Techn. J.* **30**(5), p. 749-765 (1959).
8. Kahng D., Attalla M.M. Si- SiO_2 field induced surface device // *IRE Solid State. Dev. Res. Conf.*, Pittsburg, 1960.
9. V.G. Litovchenko, A.P. Gorban'. *Physics of micro-electronic systems metal-dielectric-semiconductor*. Naukova dumka, Kiev (1978) (in Russian).
10. *Properties of the structures metal-dielectric-semiconductor*. Ed. by A.V. Rzhanov. Nauka, Moscow (1976) (in Russian).
11. V.S. Vavilov, V.F. Kiselyov, B.N. Mukashev. *Defects in silicon and on its surface*. Nauka, Moscow (1990) (in Russian).
12. A.P. Baraban, V.V. Bulavinov, P.P. Konorov. *Electron properties of SiO_2 layers on silicon*. Published in Leningrad State University, Leningrad (1988) (in Russian).
13. The physics and chemistry of SiO_2 and the Si- SiO_2 interface. // *Proc. 3 Intern. Symposium*. NJ, Pennington (1996).
14. M.L. Green, E.P. Gusev, R. Degraeve, E.L. Garfunkel, Ultrathin SiO_2 and Si-O-N dielectric layers for silicon microelectronics // *Appl. Phys. Rev.* **90**(5), p. 2057-2121 (2001).
15. P.V. Gray, D.M. Brawn, Density of Si- SiO_2 interface states // *Appl. Phys. Lett.* **8**(2), p. 31-33 (1966).
16. N.M. Johnson, Energy-resolved DLTS measurements of interface states in MIS structures // *Appl. Phys. Lett.* **34**(11), p. 802-804 (1979).
17. S.I. Kirillova, V.Ye. Primachenko, O.V. Snitko, V.A. Chernobai, Electron properties of the silicon surface in its various physico-chemical states // *Poverkhnost'* No 11, p.74-79 (1991) (in Russian).
18. S.I. Kirillova, M.D. Moin, V.Ye. Primachenko, S.V. Svechnikov, V.A. Chernobai, I.N. Dubrov, Changes of electron properties of the Si- SiO_2 system after laser irradiation // *Fizika i tekhnika poluprovodnikov* **26**(8), p. 1399-1404 (1992) (in Russian).
19. Ye.F. Venger, S.I. Kirillova, V.Ye. Primachenko, V.A. Chernobai, The system of surface electron states inherent to thermally oxidized and real silicon surfaces // *Ukrainskiy fizicheskiy zhurnal* **42**(11/12), p. 1333-1339 (1997) (in Russian).
20. S.I. Kirillova, V.Ye. Primachenko, A.A. Serba, V.A. Chernobai, The system of discrete electron states at the interface Si(100)- SiO_2 // *Mikroelektronika* **29**(5), p. 390-394 (2000) (in Russian).
21. S.I. Kirillova, V.E. Primachenko, E.F. Venger, V.A. Chernobai, Electron properties of silicon surface

- at different oxide film conditions // *Semiconductor Physics, Quantum Electronics and Optoelectronics* **4**(1), p.12-22 (2001).
22. E.H. Poindexter, MOS interface states : overview and physicochemical perspectives // *Semicond. Sci. Technol.* **4**(12), p. 961-969 (1989).
 23. G.I. Pietsch, Ubiquitous surfaces termination of the wet-chemical processing // *Appl. Phys. A* **60**(4), p. 347-363 (1995).
 24. G.F. Cerofolini, L. Meda, Chemistry at silicon crystalline surfaces // *Appl. Surf. Science* **89**(4), p. 351-360 (1995).
 25. V.Ye. Primachenko, O.V. Snitko, Physics of the semiconductor surface doped with metals. Naukova dumka, Kiev (1988) (in Russian).
 26. V.I. Beklemishev, B.G. Gribov, V.V. Levenets, I.I. Manokhin, Passivation of the silicon surface in HBF_4 // *Mikroelektronika* **24**(4), p. 315-320 (1995) (in Russian).
 27. V.V. Korobtsov, O.N. Fidyandin, A.P. Shaporenko, V.V. Balashov, Influence of the chemical treatment way on the wettability of Si(111) surface // *Zhurnal tekhnicheskoi fiziki* **66**(12), p. 134-137 (1996) (in Russian).
 28. Mechanism of HF etching of silicon surfaces: a theoretical understanding of hydrogen passivation / G. Trucks, K. Raghavachari, G. Higashi, Y. Chabal // *Phys. Rev. Lett.* **65**(4), p. 504-507 (1990).
 29. Ya. Hiroshi, Correlation between reliability and oxidation temperature for ultra-dry ultrathin silicon oxide films // *J. Electron. Mater.* **28**(4), p. 377-384 (1999).
 30. T. Akinobu, K. Kiyoteru, O. Yoshikozu et al., Highly reliable SiO_2 films formed by UV- O_2 oxidation // *Jpn J. Appl. Phys. Pt.1.* **37**(3b), p. 1122-1124 (1998).
 31. Zhang Jun-Ying, Boyd Ian W. Low temperature photo-oxidation of silicon using a xenon excimer lamp // *Appl. Phys. Lett.* **71**(20), p. 2964-2966 (1997).
 32. V.I. Sokolov, V.V. Plotnikov, A.M. Skvortsov et al., Peculiarities of thermal silicon oxidation, which are caused by structural mismatch at the interphase boundary // *Izvestiya vuzov. Elektronika.* No 5, p.17-21 (2002) (in Russian).
 33. D.K. Biegelsen, M.D. Moyer, N.M. Johnson et al., Characteristic electronic defects at the Si- SiO_2 interface // *Appl. Phys. Lett.* **43**(6), p. 563-565 (1983).
 34. G.J. Gerardi, E.H. Poindexter, P.J. Caplan, N.M. Johnson, Interface traps and P_b centers in oxidized (100) silicon wafer // *Appl. Phys. Lett.* **49**(6), p. 348-350 (1986).
 35. D. Sands, K.M. Brunson, M.H. Tayarani-Nayaran. Measured intrinsic defect density throughout the entire band gap at the Si(100) / SiO_2 interface // *Semicond.Sci.Technol.* **7**(8), p. 1091-1096 (1992).
 36. S. Ozder, I. Atilgan, B. Katircioglu. Temperature dependence of the capture cross section determined by DLTS on an MOS structure // *Semicond. Sci. Technol.* **10**(11), p. 1510-1519 (1995).
 37. A. Stesmans, B. Nouwen, V.V. Afanas'ev, ^{29}Si hyperfine structure of the P_{b1} interface defect in thermal Si(100) / SiO_2 // *J. Phys. Condens. Matter.* **10**(27), p. L.465-472 (1998).
 38. Z.S. Gribnikov, V.I. Mel'nikov, Electron-hole scattering in semiconductors at high injection levels // *Fizika i tekhnika poluprovodnikov* **2**(9), p. 1352-1360 (1968).
 39. S.I. Kirillova, V.Ye. Primachenko, V.A. Chernobai, Photomemory effect for the surface potential under various states of the silicon surface // *Optoelektronika i poluprovodnikovaya tekhnika* No 21, p. 60-63 (1991) (in Russian).
 40. V.E. Primachenko, O.V. Snitko, V.V. Milenin, Nonequilibrium field effect on Si in the region of high depletion // *Phys. status solidi* **11**(3), p. 711-718 (1965).
 41. H. Andermann, W. Henrion, M. Rebien, H-terminated silicon: spectroscopic ellipsometry measurements correlated to the surface electronic properties // *Thin Solid Films* **313/314**(5), p. 552-556 (1998).
 42. Yu.A. Novikov, A.V. Rakov, S.V. Sedov, I.B. Strizhkov, Measurements of the thickness of natural oxide on silicon by using scanning electron microscopy // *Poverkhnost' No 1*, p. 52-55 (1995).
 43. A. Stesman, V.V. Afanas'ev, Undetectability of the P_{b1} point defect as an interface state in thermal (100)Si / SiO_2 // *J. Phys. Condens. Matter.* **10**(1), p. L.19-25 (1998).
 44. T.D. Mishima, P.M. Lenehan, Do P_{b1} centers have levels in Si band gap? SDR study of P_{b1} "hyperfine spectrum" // *Appl. Phys. Lett.* **76**(25), p. 3771-3773 (2000).
 45. Y.W. Lam, Surface - state density and surface potential in MIS capacitors by surface photovoltage measurements // *J. Appl. Phys.* **42**(4), p. 1370-1379 (1971).
 46. S.I. Kirillova, V.Ye. Primachenko, V.A. Chernobai, The system of fast electron states on the real germanium surface // *Fizika i tekhnika poluprovodnikov* **30**(1), p. 118-127 (1996).
 47. O.S. Frolov. On interpretation of the field effect in germanium and silicon // *Ibid.* **1**(5), p. 784-786 (1967) (in Russian).
 48. V.F. Kiselev, S.N. Kozlov, A.V. Zoteyev, *Basics of solid surface physics.* Published in Moscow State University. Moscow (1999).
 49. I.P. Lisovsky, Investigation of the structural configuration and chemical composition of dielectric films by using the method of IR spectroscopy // *Optoelektronika i poluprovodnikovaya tekhnika* No 26, p. 93-111 (1993) (in Russian).
 50. K. Eriguchi, Y. Harada, M. Niwa, Effects of strained layer near SiO_2 -Si interface on electrical

- characteristics of ultrathin gate oxides // *J. Appl. Phys.* **87**(4), p. 1990-1995 (2000).
51. A. Szekeres, A. Paneva, S. Alexandrova, I. Lisovsky, V. Litovchenko, D. Mazunov. Optical study of ultrathin SiO₂ grown on hydrogenated silicon // *Vacuum* **69**(2), p. 355-360 (2003).
 52. W.L. Warren, J.R. Schwark, M.R. Shaneyfelt et al., Hydrogen interactions with delocalized spin center in buried SiO₂ thin films // *Appl. Phys. Lett.* **62**(14), p. 1661-1663 (1993).
 53. A. Stesmans, V.V. Afanas'ev. Annealing induced degradation of thermal SiO₂: S center generation // *Appl. Phys. Lett.* **69**(14), p. 2056-2058 (1996).
 54. A. Stesmans, V.V. Afanas'ev, Point defect generation in SiO₂ by interaction with SiO at elevated temperatures // *Microelectronic Engineering* **36**(2), p. 201-204 (1997).
 55. V.A. Gritsenko, Yu.N. Novikov, A.V. Shaposhnikov, Yu.N. Morokov, Numerical modelling of intrinsic defects in SiO₂ and Si₃N₄ // *Fizika i tekhnika poluprovodnikov* **35**(9), p.1041-1049 (2001) (in Russian).
 56. Ye.I. Verkhovsky, G.I. Yepifanov, Internal strains in silicon mono- and dioxide films // *Obzory po elektronnoi tekhnike. Ser. Poluorovodnikovyye pribory. No 9*(42), p. 1-24 (1972) (in Russian).
 57. V.P. Alekhin, *Physics of fastness and plasticity of material surface layers*. Nauka, Moscow (1983) (in Russian).
 58. Yu.A. Kontsevoi, Yu.M. Litvinov, E.A. Fattakhov, *Plasticity and fastness of semiconductor materials and structures*. Radio i svyaz, Moscow (1982).
 59. S.S. Gorelik, Yu.M. Litvinov, V.G. Postolov, A.V. Prikhod'ko, Strains created by dielectric coatings in silicon // *Elektronnaya tekhnika. Ser. Mikroelektronika. No 4*(116), p. 82-86 (1985) (in Russian).
 60. L.A. Matveeva, G.N. Semenova, L.S. Khazan, Internal mechanical strains in the Si-SiO₂ system // *Abstracts of the 2nd All-Union Conference "Physics of oxide films"*, Pt. 2, p. 5-6. Petrozavodsk, 1987.
 61. T. Brozhek, V.Ya. Kiblik, Influence of mechanical strains on electrical and radiation properties of Si-SiO₂ structures // *Optoelektronika i poluprovodnikovaya tekhnika* No 22, p. 53-62 (1992) (in Russian).
 62. N.N. Gerasimenko, V.N. Mordkovich, Radiation effects in the semiconductor-dielectric system // *Poverkhnost'*, No 6, p. 5-19 (1987) (in Russian).
 63. V.N. Ovsyuk, A.V. Rzhhanov, On quasi-continuous spectrum of levels in the forbidden band of the semiconductor surface // *Fizika i tekhnika poluprovodnikov* **3**(2), p. 294-296 (1969), (in Russian).
 64. Yu.A. Zarif'yants, V.F. Kiselev, S.N. Kozlov, Yu.F. Novototsky-Vlasov, About the energy spectrum of fast electron traps at the real semiconductor surface // *Vestnik Moscovskogo universiteta. Fizika. No 1*, p. 84-91 (1975) (in Russian).
 65. V.L. Bonch-Bruyevich, I.P. Zvyagin, R. Kaiper, *Electron theory of disordered semiconductors*. Nauka, Moscow (1981) (in Russian).
 66. P.I. Grunthaner, F.J. Grunthaner. High-resolution x-ray photoelectron spectroscopy as a probe of local atomic structure // *Phys. Rev. Lett.* **43**(22), p. 1683-1686 (1979).
 67. R.B. Laughlin, J.D. Joannopoulos, D.J. Chadi, Theory of the electronic structure of the Si-SiO₂ interface // *Phys. Rev. B* **21**(12), p. 5733-5744 (1980).
 68. E. Martinex, F. Yndurain, Possibility of intrinsic Si states localized at the Si-SiO₂ interface // *Phys. Rev. B* **25**(10), p. 6511-6513 (1982).
 69. D. Pierreux, A. Stesmans, Interface strain in thermal Si(111)-SiO₂ analysed by frequency dependent electron spin resonance // *Physica B* **308-310**(4), p. 481-484 (2001).
 70. H. Kageshima, K. Shiraishi, Microscopic mechanism for Si/SiO₂ interface passivation : Si=O double bond formation // *Surface Science* **380**(1), p. 61-65 (1997).
 71. V.V. Afanas'ev, A. Stesmans, Blockage of the annealing-induced Si / SiO₂ degradation by helium // *Appl. Phys. Lett.* **74**(7), p. 1009-1011 (1999).
 72. A. Stesmans, Comparative analysis of the H₂ passivation of interface defects at the (100)Si / SiO₂ interface using ESR // *Solid State Commun* **97**(4), p. 255-259 (1996).
 73. A. Stesmans, Reversion of H₂ passivation of P_b interface defects in standart (111)Si / SiO₂ // *Appl. Phys. Lett.* **68**(19), p. 2723-2725 (1996).
 74. L.D. Thanh, P. Balk, Elimination and generation of Si / SiO₂ interface traps by low temperature hydrogen annealing // *J. Electrochem. Soc.* **135**(7), p. 1797-1801 (1988).
 75. G.V. Gadiyak, Physical model and numerical results of dissociation kinetics of hydrogen-passivated Si/SiO₂ interface defects // *Thin Solid Films.* **350**(1/2), p. 147-152 (1999).
 76. E. Cartier, J.H. Stathis, D.A. Buchanan, Passivation and depassivation of silicon dangling bonds at the Si/SiO₂ interface by atomic hydrogen // *Appl. Phys. Lett.* **63**(11), p.1510-1512 (1993).
 77. R.E. Stahlbush, Slow and fast state formation caused by hydrogen // *Proc. 3 Intern. symposium "The physics and chemistry of SiO₂ and the Si-SiO₂ interface"*. Pennington, NY: 1996. Vol.96-1, p. 525-537.
 78. V.V. Afanas'ev, A. Stesmans, Positively charged bonded states of hydrogen at the (111)Si / SiO₂ interface // *J. Phys.:Condens. Matter.* **10**(1), p. 89-93 (1998).
 79. L.G. Gosset, J.J. Ganen, H.J. Bardeleben et al., Formation of modified Si / SiO₂ interfaces with intrinsic low defect concentrations // *J. Appl. Phys.* **85**(7), p. 3661-3665 (1999).
 80. Ha Yong Ho, Kim Schum, Lee Sun Young et al., Relaxation of the Si lattice strain in the Si(100)-SiO₂

- interface by annealing in N_2O // *Appl. Phys. Lett.* **74**(23), p. 3510-3512 (1999).
81. X. Chen, J.M. Gibson, Roughness at Si / SiO_2 interfaces and silicon oxidation // *J. Vac. Sci. Technol. A* **17**(4), Pt.1, p. 1269-1274 (1999).
82. L. Lai, K.J. Hebert, E.A. Irene, A study of the relationship between Si/ SiO_2 interface charges and roughness // *J. Vac. Sci. Technol. B* **17**(1), p. 53-59 (1999).
83. T. Brozhek, V.Ya. Kiblik, V.G. Litovchenko et al., *Radiation-enhanced effects in layered MDS structures*. Preprint No 4-88 of the Institute for Semiconductors, Academy of Sciences of Ukraine. Kiev, 1988.
84. F.J. Grunthner, P.J. Grunthner, J. Maserijon, Radiation induced defects in SiO_2 as determined by XPS // *IEEE Trans. Nucl. Sci.* **29**(6), p. 1462-1466 (1982).
85. F.J. Grunthner, P.J. Grunthner, Chemical and electronic structure of Si/ SiO_2 interface // *Mat. Sci. Rep.* No 2/3, p. 65-160 (1986).
86. P.M. Lenahan, P.V. Dressendorfer, Microstructural variations in radiation hard and soft oxides observed through ESR // *EEE Trans. Nucl. Sci.* **30**(6), p. 4602-4604 (1983).
87. N. Haneji, L. Vishnubhota, T.P. Ma, Possible observation of P_{b0} and P_{b1} center at irradiated (100)Si/ SiO_2 interface from electrical measurements// *Appl. Phys. Lett.* **59**(26), p. 3416-3418 (1991).
88. P.M. Lenahan, T.D. Mishima, T.M. Fogarty, R. Wilkins, Atomic- scale processes involved in long-term changes in the density of state distribution at the Si/ SiO_2 interface // *Appl. Phys. Lett.* **79**(20), p. 3266-3268 (2001).
89. M.N. Levin, Ye.N. Bormontov, O.V. Volkov, S.S. Ostroukhov, A.V. Tatarintsev, Enhanced generation of surface states in MDS-elements of intergrated circuits after action of UV and X-ray radiations // *Mikroelektronika* **30**(1), p. 16-21 (2001).
90. S.K. Boitsov, A.Ya. Vul', A.T. Dideykin et al., Processes of current transfer through tunnel-transparent dielectric of STDS structures // *Fizika tverdogo tela* **33**(6), p. 1784-1791 (1991) (in Russian).
91. L.Do Thanh, M. Aslam, P. Balk, Defect structure and generation of interface states in MOS structures // *Solid State Electronics* **29**(8), p. 829-840 (1986).
92. T.B. Hook, T.P. Ma, Hot electron induced interface traps in MOS capacitors // *Appl. Phys. Lett.* **48**(18), p. 1208-1210 (1986).
93. W.D. Zhang, J.F. Zhang, M.J. Uren et al., On the interface states generated under different stress condition // *Appl. Phys. Lett.* **79**(19), p. 3092-3094 (2001).
94. S. Ogawa, N. Shiono, Interface-trap generation induced by hot-hole injection at the Si- SiO_2 interface // *Appl. Phys. Lett.* **61**(7), p. 807-809 (1992).
95. S. Kar, Ultimate gate oxide thinness set by recombination tunneling of electrons via Si- SiO_2 interface traps//*J. Appl. Phys.* **88**(5), p. 2693 (2000).